Scaling the solute transport characteristics of surcharged manholes

S. Lau*, V. Stovin* and I. Guymer**

*Department of Civil and Structural Engineering, The University of Sheffield, Mappin Street, Sheffield, S1 4DT, UK
(Email: s.lau@sheffield.ac.uk; v.stovin@sheffield.ac.uk)
**School of Engineering, University of Warwick, Coventry, CV4 7AL, UK
(Email: i.guymer@warwick.ac.uk)

Abstract Guymer *et al.* (2005) presented the results of experimental work that explored the effects of diameter and surcharge on the solute transport processes occurring in surcharged manholes. A threshold surcharge level was identified, with two contrasting hydraulic regimes being observed at surcharge depths above and below the threshold value. In this study, a 1:3.67 physical scale model of an 800 mm diameter manhole has been built to investigate the effects of scale on hydraulic and solute transport characteristics. Dye tracing experiments and energy loss measurements have been made in the physical scale model. The results suggest that geometrical scaling laws may be used to characterise the flow regime, and to identify the threshold surcharge depth. Solute transport characteristics are presented in the form of a cumulative Residence Time Distribution (RTD) curve, in which the x-axis (time dimension) is normalised by the nominal residence time (volume/discharge). The RTD curves reveal the effect of hydraulic regime on solute transport processes, with two distinct characteristic curve shapes corresponding to the two contrasting hydraulic regimes. A preliminary comparison of the normalised RTD curves for the model and prototype systems suggests that the scale-independent solute transport characteristics of the structure may be characterised by just two dimensionless RTD curves; one for pre-threshold and the second for post-threshold hydraulic conditions.
Keywords Dispersion, energy loss, hydraulic regime, manhole, residence time distribution (RTD), sewer, solute transport, surcharge

Introduction

Solute transport processes affect the performance of a wide range of water engineering structures. In the context of urban drainage, future legislation (certainly in Europe) is likely to focus increasingly on the effects of dissolved pollutants. The effects of dispersion may act to reduce or eliminate first foul flush effects or to moderate peak concentrations associated with intermittent discharges. Dispersion also implies that pollutant materials may be present a long time before and after predictions based on mean travel time would suggest. Urban drainage network models that predict the transport of dissolved substances are increasingly used. Some of the models transport the pollutants by advection only, while others also account for the effects of dispersion. At present there is limited knowledge regarding appropriate values for the model parameters. In some instances laboratory measurements have been conducted (see e.g. Guymer *et al.,* 2005), but the applicability of laboratory-scale derived parameters to full-scale structures in the urban drainage system, i.e. scalability of these parameters, is not clearly understood.

Guymer *et al.* (2005) presented comprehensive data from laboratory experiments on the travel times and dispersion associated with a solute pulse passing through a surcharged manhole. Of particular interest in this work was the identification of a threshold surcharge level at which the solute transport characteristics indicate a sharp transition between pre- and post-threshold levels. At surcharge levels below the threshold, the travel times increase linearly with surcharge, whilst above the threshold travel times drop to a low and constant value. A Computational Fluid Dynamics-based study was conducted to investigate the underlying flow mechanisms that governed these mixing characteristics (Lau *et al.*, 2006). Results have shown two distinct hydraulic regimes in the manhole; pre-threshold the flow field is dominated by a chaotic and swirling motion throughout the manhole volume that promotes full mixing; whilst post-threshold the flow field comprises two separated flow regimes – a dead zone is formed in the upper volume of fluid, which the majority of the incoming flow passes beneath.

The present study aims to investigate how scaling affects both the hydraulic and solute transport characteristics of surcharged manholes. A 1:3.67 physical scale model of the 800 mm diameter manhole (prototype) has been constructed, and solute transport experiments have been undertaken to evaluate the travel time and dispersion characteristics. The present work also quantifies the

effects of discharge and surcharge on energy loss for this particular manhole configuration (ratio of manhole diameter to pipe diameter), which has not been published in previous manhole studies (O'Brien, 1999; Dennis, 2000; Guymer *et al.*, 2005).

Experimental Facilities and Procedure

The self-contained recirculating system used for this study is similar to the one described in Guymer and O'Brien (2000). It comprised a constant header tank and a storage sump from which a submersible pump continuously circulated water through the system. The system had a maximum discharge capacity of 16 l/s and the flow rate through the test section (Figure 1) was controlled by a discharge control valve 4 m upstream of the manhole. The test section consisted of a horizontal Perspex pipe 24 mm internal diameter (ID) and a 218 mm ID manhole. The discharge through the manhole apparatus was monitored using a Venturi meter installed 1.24 m downstream of the manhole outlet. This measurement device was connected to two 25 mm diameter manometers with a measurement scale attached. The flow rate measurement system was calibrated in-situ using a volumetric method and could quantify a range of flow rates from 0.1 to 2 l/s with an accuracy to 0.01 l/s. Positioned at the end of the pipe exit was a surcharge control system. The entrance of the system was positioned at a lower elevation level compared with that of the manhole exit. This was to provide sufficient head between the water levels in the manhole and in the surcharge tank such that a complete range of surcharges could be studied. The water level in the manhole was controlled by modifying the weir height in the tank. Temporal variations in free water surface within the manhole were recorded using a model H45 water level follower (Armfield). This device could measure water level changes up to 50 mm/s.

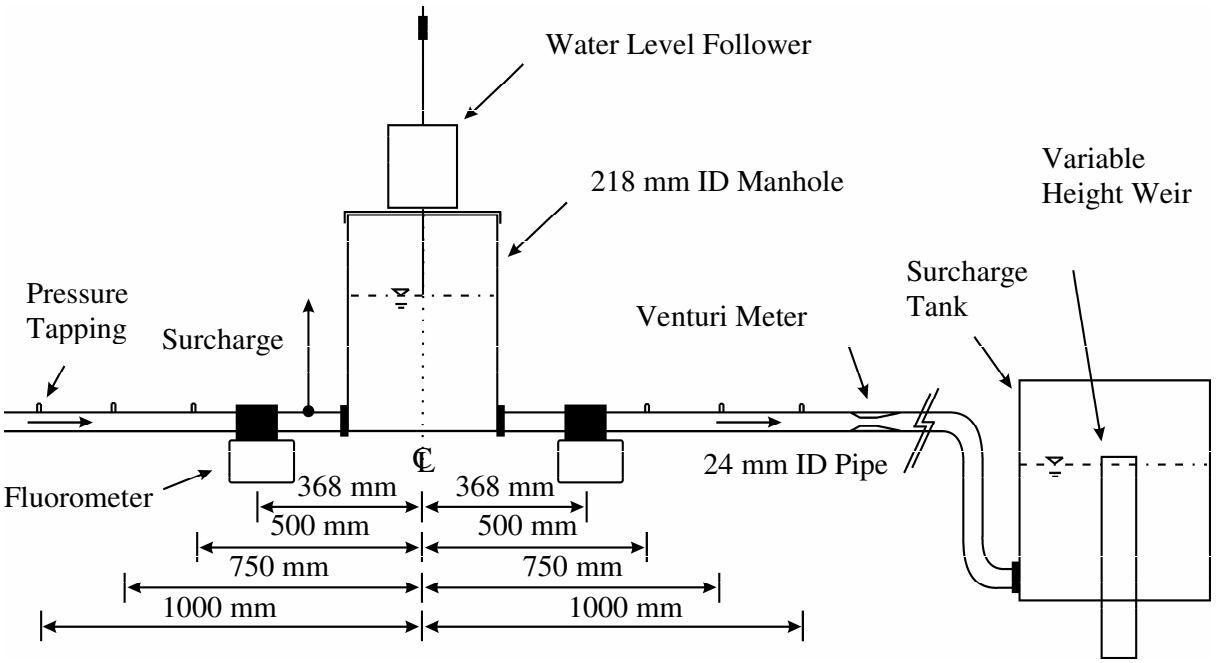

Figure 1 – Experimental configuration

Series 10 fluorometers (Turner Designs) were used to monitor temporal concentration distributions at the sampling stations, which were situated 368 mm upstream and downstream from the manhole centre. The fluorometers were slightly modified to allow the 30 mm outer diameter, (24 mm ID) Perspex pipe to fit the instrument's original configuration for non-intrusive continuous sampling. With this setting the pipe cross sectional concentration was determined without any flow disturbance. In this configuration, the Turner Designs fluorometers are highly susceptible to interference from extraneous light that may intrude into the sampling section. As a result, all

pipework and the manhole were fully enclosed with wooden black-out boxes. The two fluorometers were calibrated in-situ following the procedure suggested by O'Brien (1999). Rhodamine WT was used for the dye tracing experiments. The fluorometers were regulated to operate in the linear response region up to dye concentrations 2.5 x 10^{-7} l/l. In each test run, approximately 25 ml of the dilute solution was introduced in the form of an instantaneous injection into the supply pipe 4 m upstream of the upstream sampling station. This distance, more than 100 pipe diameters, ensured that the solute concentration was cross-sectionally well mixed (approximately Gaussian distribution) at the upstream measurement position.

Six pressure tappings were installed at 500, 750 and 1,000 mm upstream and downstream from the centre of the manhole. The closest downstream tapping point was about 16 pipe diameter downstream of the manhole outlet, at which point it would be expected that a fully turbulent flow profile would have re-established (generally accepted minimum distance is 10 pipe diameters (Howarth, 1985)). Each tapping was connected to an 88 mm diameter stilling column with a measurement scale that could be read to an accuracy of 1 mm.

In the scale model study, five flow rates between 0.25 to 0.5 l/s and ten surcharge depths within the range of 10 and 100 mm have been considered, resulting in five hundred steady flow hydraulic conditions. In each case study, 5 repeat runs were performed. In each run, digital readings from the fluorometers and the water level follower were logged simultaneously at 50 Hz for a period of 5 minutes. The time to peak was generally less than 5 s; in all cases the solute concentration at the downstream measurement position had returned to background levels well within the 5 minute cut-off. For the pressure measurement, the manometer readings were recorded three times during each run.

Data Analysis

For each individual injection of solute tracer, temporal concentration distributions were recorded from both upstream and downstream fluorometers. The data captured from the fluorometers were purely digital signals and required post-processing to determine the concentration distributions corresponding to the solute. The post-processing procedure comprised calibration, background concentration removal and identification of the start and end points of temporal concentration distributions, i.e. to eliminate noisy background data. The technique for the first two processes is well-established (see e.g. O'Brien, 1999; Dennis 2000). However, several techniques have been proposed for the identification of the profile start and end points. Dennis (2000) defined the cut-off as the 10^{th} consecutive data point away from the peak with a concentration value less than 1 % of the peak concentration. This technique was tested on the temporal concentration distributions obtained from a straight pipe study. The study employed the same laboratory configuration as Figure 1 but with a 24 mm ID straight pipe replacing the manhole. Results showed that the cut-off technique successfully eliminated the noisy background, whilst keeping the entire solute trace (mass balances of above 99%). This cut-off technique was therefore applied to all manhole tracer profiles.

In this paper, the travel time is defined in terms of the cumulative residence time distribution. The median travel time (50^{th} percentile), defined as the time difference between the 50^{th} percentile of the upstream and downstream profiles, has been adopted to represent the characteristic travel time of the system.

Under steady hydraulic conditions, variations in pressure and surcharge level during the experiment were insignificant. Pressure fluctuations shown on the manometers were within ± 1 mm of the mean value. The measurements from the water level followers showed a mean standard deviation during each test of 2 mm over the range of surcharge depths studied, with greater fluctuations being observed at low surcharge depths. In certain circumstances, where the free surface in the manhole fluctuated about a mean depth at high frequency, the water level follower failed to track the surface and gave faulty readings, for example a signal reading corresponding to a negative surcharge level. These faulty readings were eliminated before averaging the water level data series.

The energy loss coefficient for the surcharged manhole was estimated from the pressure measurements. The head loss due to the manhole, ΔH, is defined as the difference in pressure head at the manhole centreline between the extrapolated upstream and downstream hydraulic lines, obtained from 3 points measurement. Values of the coefficient were calculated using the equation below:

$$\Delta H = K \frac{u^2}{2g} \tag{1}$$

where u = mean pipe velocity; g = gravitational acceleration; and K= head loss coefficient.

Results

Relationship between energy loss coefficient and surcharge ratio

The surcharge ratio is defined as the ratio of surcharge depth (measured with respect to the soffit of the pipe) to manhole diameter, S. The variations of energy loss coefficient with surcharge ratio for the 218 mm diameter manhole are shown in Figure 2. A sharp transition of the energy loss coefficient between pre- and post-threshold is evident at a surcharge ratio of between 2 and 2.5. At surcharge ratios below the threshold ratio, energy loss coefficients appear to increase with surcharge ratio, although the rate of increment is slow. At the lowest surcharge ratio, there are several data points that fall below the linear trend, with values less than 0.9. This phenomenon is similar to the one observed in Arao and Kusuda (1999), shown in Figure 3; immediately after the manhole was surcharged, in the range of 0 to 0.5 surcharge ratio, energy loss coefficients increased rapidly with surcharge; beyond this region, the rate of increase began to flatten off. Figure 2 shows that the hydraulic transition has a significant impact on energy loss. After the transition, the coefficient values are reduced by half compared with the values in the pre-threshold region, yielding a coefficient value of around 0.45.

The threshold depth for the hydraulic transition differs between the present data set and that presented by Arao and Kusada (1999) (surcharge to pipe diameter ratio of 2.5 compared with 1). This reflects the fact that the two studies have considered manholes with different manhole diameter to pipe diameter ratios. Guymer *et al*. (2005) suggested that the threshold depth varies as a linear function of the manhole diameter to pipe diameter ratio, and that the value of the threshold depth can be approximately predicted by reference to jet theory.

The relationship between energy loss coefficient and surcharge ratio observed in the post-threshold region matches well to the experimental findings in Arao and Kusuda (1999). Immediately after the hydraulic transition, the coefficient values decrease significantly and remain constant. Figure 3 suggests that a secondary peak in energy loss occurred at surcharge ratios of around 3.3 (i.e. three times the surcharge ratio associated with the primary step in energy loss coefficient). As the present laboratory data set does not extend beyond two times the threshold surcharge ratio, it is not possible to comment on the existence or not of a comparable secondary peak. Energy loss does not appear to be strongly dependent upon discharge.

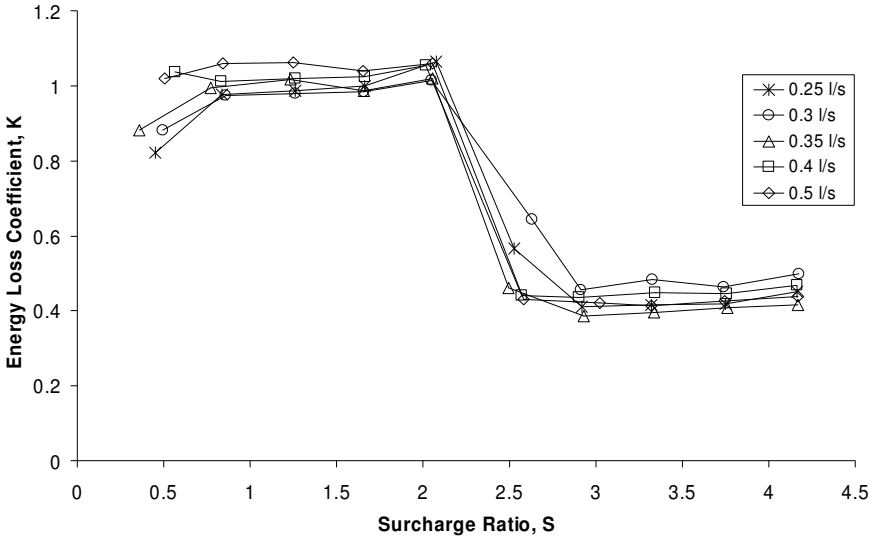

Figure 2 – Variations of energy loss coefficient with surcharge ratio for the 218 mm diameter manhole

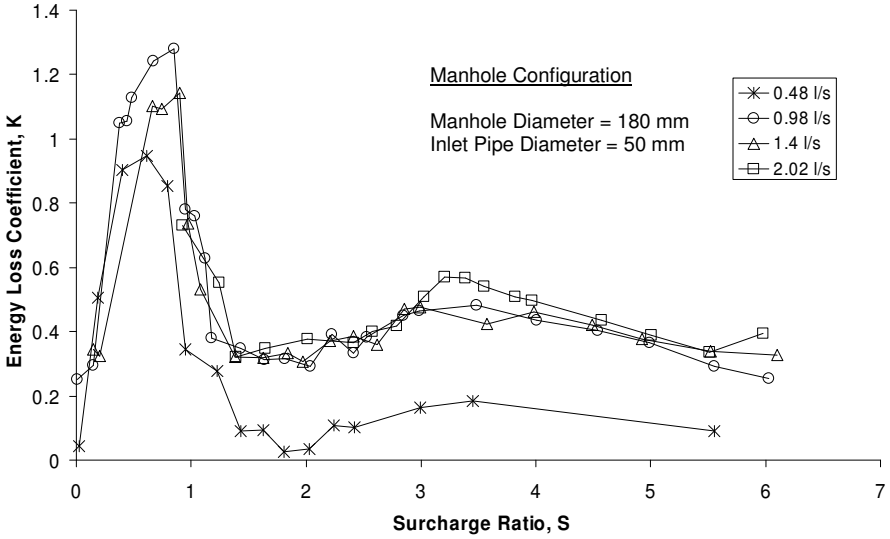

Figure 3 - Relationship between head loss coefficient and surcharge ratio (After Arao and Kusuda, 1999)

Relationship between travel time and surcharge ratio

Values of the median travel time for the scale model are presented in Figure 4. The travel time results show similarity to the results presented in Guymer *et al.* (2005) (figure not shown). A sharp transition at a surcharge ratio of between 2 and 2.5 can be clearly identified in the 218 mm diameter manhole data, whereas the threshold surcharge ratio observed in Guymer *et al.* (2005) was approximately 2.5. In the pre-threshold region, travel times vary linearly with surcharge; whilst post-threshold, travel times drop to a low and nearly constant value. In addition, both results demonstrate an inverse relationship with discharge.

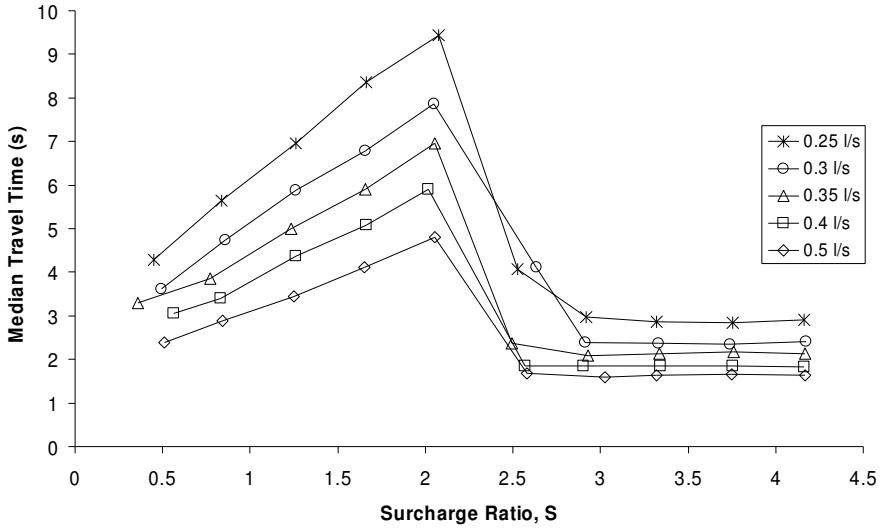

Figure 4 – Relationship between median travel time and surcharge ratio for the 218 mm diameter manhole

Discussion

Temporal concentration distributions comparison – prototype and scale manhole

The travel time data for the scale model suggest that the scale model showed similar hydraulic characteristics to the prototype presented in Guymer *et al.* (2005). The threshold depth occurred at a comparable surcharge to pipe diameter ratio, confirming the validity of geometric scaling. Figures 5a and b present comparisons of the downstream distributions in response to an upstream Gaussian concentration. For comparative purposes, the distributions are normalised with respect to the peak concentration and the downstream temporal concentration distributions are plotted from time zero. The trends in the variation of downstream distribution shape as a function of surcharge are highly comparable in both manhole models. Normalised with respect to the peak, the distributions show no noticeable difference at the rising limbs. The effects of surcharge on the distributions become marked in the shape of the falling limb. In all distributions, the Gaussian-like profile distorts at some point and follows an approximate linear decay. Pre-threshold, the concentration at which the distortion commences appears to increase with surcharge; whilst post-threshold, the distortion begins at comparatively lower concentration levels and the surcharge level appears to have no influence on the concentration at which the distortion commences.

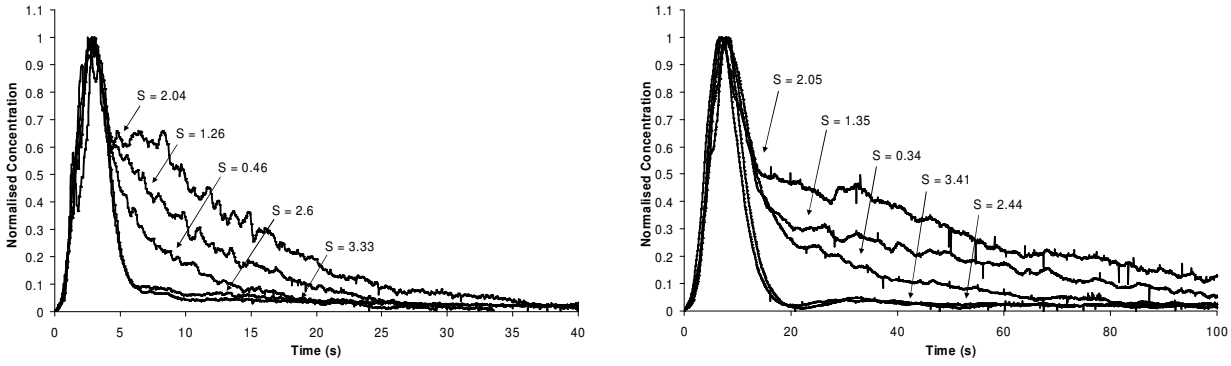

(a) (b)

Figure 5 – Effects of variations in surcharge on downstream temporal concentration distributions: (a) the scale model operated at 0.3 l/s; (b) the prototype operated at 2 l/s, after Guymer *et al.* (2005)

Comparison of cumulative retention time distributions – prototype and scale model

The scalability of the solute transport characteristics is studied via the comparison of cumulative retention time distributions (RTDs), shown in Figures 6 and 7 for pre- and post-threshold respectively. The distributions presented in the figures are the cumulative downstream profiles with the y-axis normalised with respect to the total mass of the corresponding upstream distribution and the time axis with nominal travel time, t_n (the total water volume between sampling stations divided by discharge). For presentation purposes, only one surcharge depth is considered for each hydraulic regime; the sample depths have been selected to represent a mid-point from the pre-threshold depth range ($S \approx 1.3$, Figure 6) and a mid-point from the post-threshold dataset ($S \approx 3.3$, Figure 7).

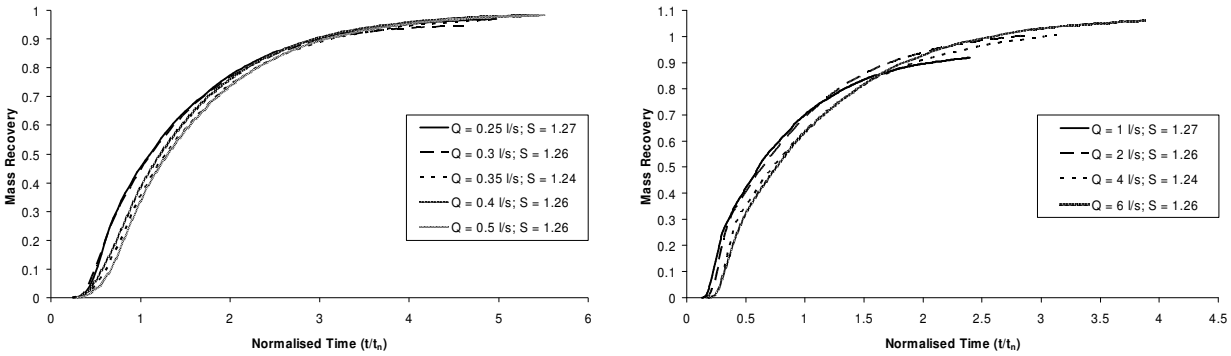

(a) the scale model (b) the prototype

Figure 6 – Comparison of pre-threshold cumulative retention time distributions for the manholes

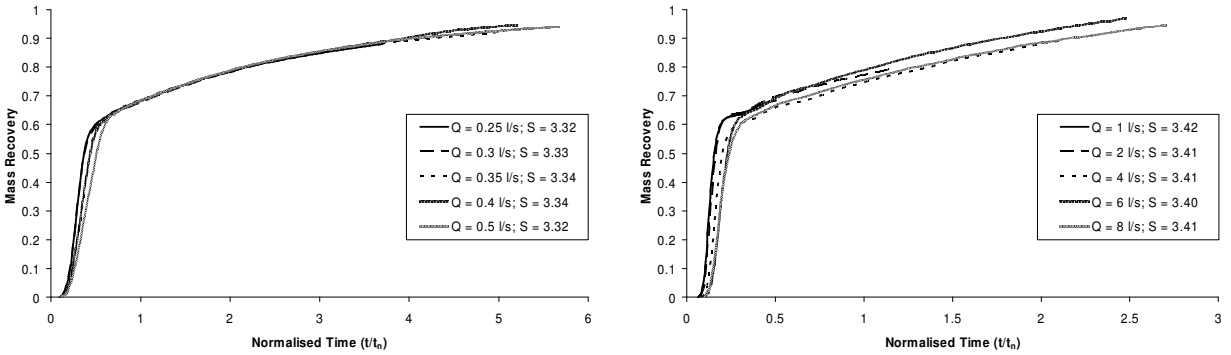

(a) the scale model (b) the prototype

Figures 7 – Comparison of post-threshold cumulative retention time distributions for the manholes

It is evident that, after normalisation, the distributions in each figure tend to collapse onto a single curve, and that no systematic variation arises as a function of discharge. The plots corresponding to different surcharge depths within the same hydraulic regime (not shown) also fall on the same single characteristic curve, implying that the effects of both discharge and surcharge are accounted for in the temporal normalisation process.

Comparison of Figure 6a and b suggests that the basic shape of the pre-threshold RTD curve is constant, irrespective of manhole scale. The exponential curve indicates instantaneous mixing.

Post-threshold (Figures 7a and b), the downstream distributions reflect a different mixing mechanism. The cumulative concentration distributions appear to consist of two sections, a symmetrical (i.e. Gaussian) profile between mass recovery 0 % to about 65 % and an approximately linear tail from 65 % onwards. The steep slope immediately after the first arrival of the trace indicates that short-circuiting affects 65 % of the injected tracer. The rest of the tracer, which has been trapped in the manhole, is released at a relatively slow rate. For example, to achieve 90 % of

mass recovery, it could take more than four times the normalised median travel time. Note that complete mass recovery was not attained in most of the RTDs. Loss of mass could result from the cut-off scheme applied to the profiles and, more probably, the instrumental noise of the fluorometers at low concentrations. As in the pre-threshold hydraulic regime, comparison of Figures 7a and 7b suggests that the basic shape of the normalised RTD curve is scale-independent.

The analysis presented above suggests that the solute transport characteristics of the surcharged manhole can be summarised in terms of just two cumulative RTD curves, one for each of the two identified hydraulic regimes. However, more careful examination of Figures 6a and b and 7a and b suggests that the curves derived from the two different experimental scale models do not exactly coincide. This is likely to reflect the fact that the characteristics of the upstream distribution (i.e. its shape and duration) differed between the two experimental data sets, and work is underway to generate RTD curves that correspond to instantaneous upstream profiles. Any discrepancies that remain will then need to be accounted for as scale effects for the manhole system.

Conclusions

A 1:3.67 physical scale model of an 800 mm diameter manhole has been constructed and experiments have been undertaken to examine its hydraulic and solute transport characteristics. The energy loss coefficient and the median travel time for the 218 mm manhole show a sharp transition between pre- and post-threshold surcharge depth, and the transition appears at a surcharge ratio of between 2 and 2.5. This ratio matches that observed in an 800 mm manhole, confirming that geometric scaling on the threshold depth is valid.

Scale effects on solute travel time and dispersion characteristics have been considered via the comparison of cumulative RTDs. The cumulative normalised RTDs for each manhole collapse onto a single curve for each of the two hydraulic regimes. The normalised RTDs of the two manhole models also appear to be similar in terms of profile shape, which suggests that the two RTD curves could provide a scale-independent method of characterising the travel time and dispersion characteristics for this type of system. Further work is required to eliminate the influence of upstream concentration profiles in order to verify this hypothesis.

References

Arao, S. and Kusuda, T. (1999). Effects of Pipe Bending Angle on Energy Losses at Two-Way Circular Drop Manholes. *8th Intl. Conf. On Urban Storm Drainage*, 30 Aug. – 3 Sept., Sydney, Australia, 2163-2168.

Dennis, P. M. (2000). Longitudinal Dispersion due to Surcharged Manholes. PhD Thesis, The Univ. of Sheffield, Sheffield, U.K.

Guymer, I., and O'Brien, R. T. (2000). Longitudinal Dispersion due to Surcharged Manhole. *J. Hydraul. Eng.*, Vol 126, No.2, 137-149.

Guymer, I., Dennis, P. M., O'Brien, R. T. and Saiyudthong, C. (2005). Diameter and Surcharge Effects on Solute Transport across Surcharged Manholes. *J. Hydraul. Eng.*, Vol 131, No.4, 312-321.

Howarth, D. A. (1985). The Hydraulic Performance of Scale Model Storm Sewer Junctions. PhD Thesis, The University of Manchester, Manchester, U.K.

Lau, S. D., Stovin, V. and Guymer, I. (2006). The Prediction of Solute Transport in Surcharged Manholes using CFD. *Proc. 7th Int. Conf. on Urban Drainage Modelling and 4th Int. Conf. on Water Sensitive Urban Design*, 2-7 April 2006, Melbourne, Australia, Vol. 1, 51-58.

O'Brien, R. T. (1999). Dispersion due to Surcharged Manholes. PhD Thesis, The Univ. of Sheffield, Sheffield, U.K.